A Supramolecular Cytochrome P450 Mimic

Albertus P. H. J. Schenning, Jeffrey H. Lutje Spelberg, Dominicus H. W. Hubert, Martinus C. Feiters,* and Roeland J. M. Nolte*

Abstract: An amphiphilic rhodium(III) complex has been incorporated in closed bilayers of surfactants with positive, zwitterionic, or negative charges. In the presence of formate this rhodium complex efficiently catalyzes the reduction of a variety of electron carriers and manganese(III) porphyrins. The charge of the surfactant head groups determines the acidity of the reduced Rh^{III} hydride complex and the rate of reduction, which increases on going from negatively to positively charged surfactants. A manganese(III) porphyrin, incorporated in the bilayers together with the Rh complex, can be used as an artificial cytochrome P450-type epoxidation catalyst. The relative concentrations of Mn^{II} and Mn^{III} porphyrin depend on the reduction and reoxidation rates, and an oscillating reaction is observed at a Rh complex/Mn porphyrin ratio of 10. A variety of substrates are epoxidized by reductive activation of O_2 by this model system with turnover numbers of the same order of magnitude as those of the enzyme system. The charge on the surfactant has a dramatic effect on the catalytic epoxidation activity of the model system. Aggregates of positively charged surfactant molecules do not display catalytic activity in this reaction, probably because the protons required for cleavage of the oxygen–oxygen bond are repelled at the aggregate surface.

Keywords: enzyme mimetics · epoxidations · O–O activation · porphyrinoids · vesicles

Introduction

Cytochrome P450 catalyzes a variety of oxidation reactions, including the hydroxylation of alkanes and the epoxidation of alkenes according to Equation (1).[1] The active site of this

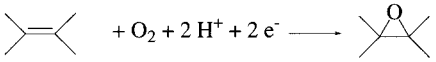

(1)

membrane-bound enzyme contains a heme function with a thiolate as axial ligand. The catalytic cycle involves the binding of a substrate, reduction of iron(III) to iron(II), and binding and reductive cleavage of molecular oxygen to generate formally an iron(V) oxo complex, which transfers its oxygen atom to the bound substrate. The iron center accepts the electrons from NADPH with mediation of a cytochrome P450 reductase. Temporary association of this flavo reductase protein with cytochrome P450 facilitates a fast two-electron transfer that is important for an efficient epoxidation reaction (Figure 1).[2] After the formation of the iron oxo species, the reductase–cytochrome P450 complex dissociates, interrupting the supply of electrons. This inhibits the unproductive water-forming pathway (Figure 1B). The protons necessary for the cleavage of the bound oxygen are presumably derived from complexed water molecules.[2]

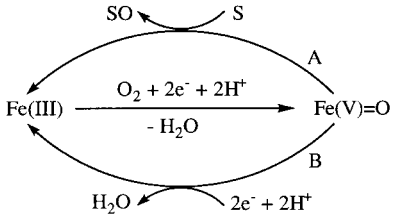

Figure 1. Substrate oxidation by cytochrome P450. Consumption of iron(v) oxo complex by substrate (S) oxidation (productive pathway, A) and the nonproductive pathway, which yields water as the product (B).

Because of its biologically crucial role in the metabolism of endogeneous chemicals and xenobiotics and also because this archetypal oxidation catalyst may serve as a model for a new generation of synthetic catalysts, much research has focused on mimicking the action of cytochrome P450.[3] Systems containing metalloporphyrins in combination with a single oxygen donor such as iodosylarenes, H_2O_2, NaOCl, and peracids have been successfully used for the oxidation of substrates.[4] Metalloporphyrin systems with O_2 as an oxygen source in combination with a reducing agent such as ascorbic

[*] Prof. Dr. R. J. M. Nolte, Dr. M. C. Feiters, Dr. A. P. H. J. Schenning, J. H. Lutje Spelberg, D. H. W. Hubert
Department of Organic Chemistry, NSR Center
University of Nijmegen, Toernooiveld
NL-6525 ED Nijmegen (The Netherlands)
Fax: (+31) 24-3652929

  0947-6539/98/0405-0871 $ 17.50+.25/0

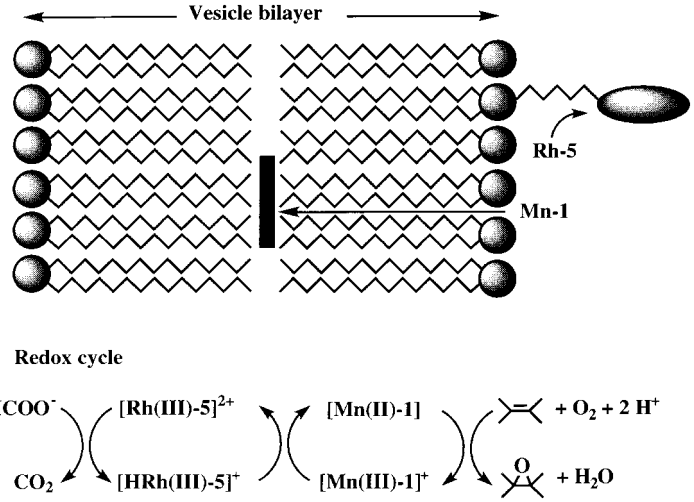

Figure 2. Schematic representation of the supramolecular cytochrome P450 mimic.

acid, H_2/Pt, Zn, or borohydride have also been described.[5] Until now, however, only a few models are known that contain all the important components of the natural system: molecular oxygen as oxidizing agent, a metalloporphyrin as catalyst, an electron donor as reducing agent, and a membrane system that holds these components together.[6–8] All these models have displayed very low catalytic activity.

In our studies on supramolecular catalytic systems, we found that the rhodium complex $[Rh^{III}(\eta^5\text{-Cp*})(bipy)Cl_2]$ (Cp*H = pentamethylcyclopentadiene, bipy = 2,2′-bipyridine) is an efficient catalyst for the reduction of manganese(III) porphyrins by sodium formate.[9] This finding allowed us to develop a new membrane-bound cytochrome P450 mimic that incorporates most of the features of the natural enzyme system: 1) a membrane-bound metalloporphyrin (M = Mn), 2) an axial ligand (*N*-methylimidazole), 3) an electron donor (**Rh-5**/formate), 4) molecular oxygen as oxygen donor, and 5) a membrane system that holds the components within its bilayer (Figure 2).[10] This so-called microreactor epoxidizes alkenes with the highest turnover numbers reported so far for membrane-bound model systems.

Abstract in Dutch: *Een amfifiel rhodium(III) complex is ingebouwd in gesloten bilagen van surfactanten met positieve, zwitterionische, of negatieve lading. In aanwezigheid van formiaat katalyseert dit rhodiumcomplex op efficiente wijze de reductie van een aantal elektronen-carriers en mangaanporfyrines. De lading van de surfactantkopgroepen bepaalt zowel de zuursterkte van het gereduceerde Rh^{III}-hydride complex als de reductiesnelheid, die toeneemt gaande van negatief naar positief geladen surfactanten. Een mangaan(III)porfyrine dat met het Rh-complex in de bilagen is ingebouwd, kan gebruikt worden als een kunstmatige cytochroom-P450-achtige katalysator voor epoxidatie. De relatieve concentraties van Mn^{II}- en Mn^{III}-porfyrines hangen af van de reductie- en reoxidatie-snelheden, en bij een verhouding Rh-complex:Mn-porfyrine van 10 wordt een oscillerende reactie waargenomen. Diverse substraten worden geëpoxideerd door reductieve activering van O_2 met dit modelsysteem met omzettingssnelheden die van dezelfde orde van grootte zijn als die van het enzymsysteem. De lading van het surfactant heeft een dramatisch effect op de katalytische epoxidatieactiviteit van het model. Aggregaten van positief geladen surfactanten vertonen geen katalytische activiteit in deze reactie, waarschijnlijk omdat de protonen die nodig zijn voor de splitsing van de zuurstof-zuurstof-binding door het aggregaatoppervlak worden afgestoten.*

Results and Discussion

Incorporation: The porphyrin catalysts **Mn-1**, **Mn-2**, **Mn-3**, **Mn-4**, and the rhodium co-catalyst **Rh-5** were synthesized and characterized as described in the Experimental Section. Except for **Mn-4**, these compounds were incorporated in bilayers of DPPC, DPPA, DHP, and DODAC vesicles by the ethanol/THF injection method,[11] and incorporation was confirmed by gel permeation chromatography (GPC). Electron microscopy showed that after incorporation of the

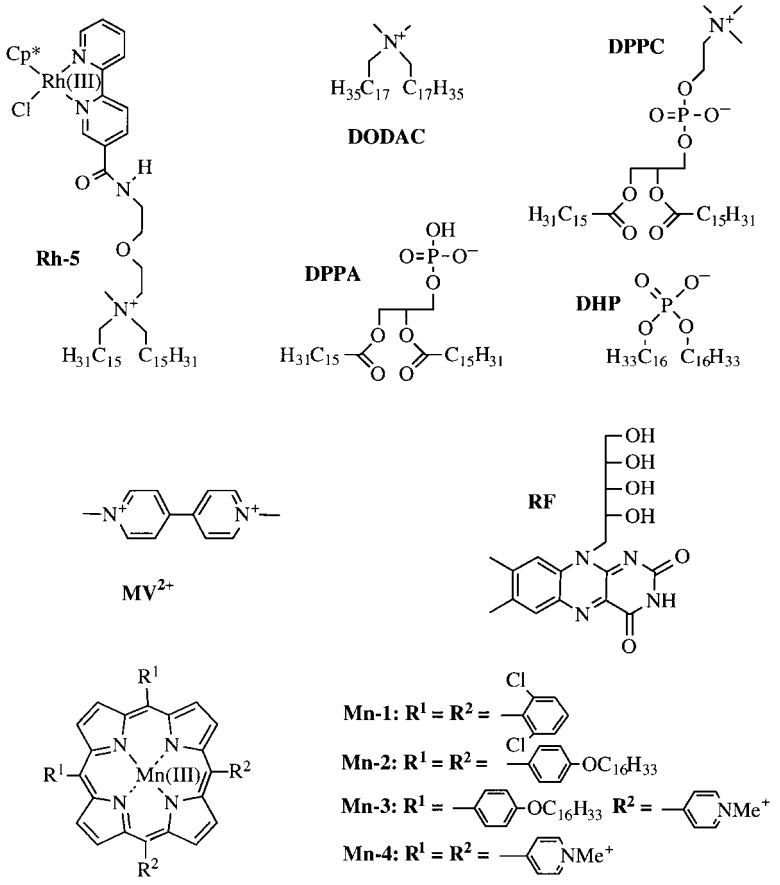

0947-6539/98/0405-0872 $ 17.50+.50/0 *Chem. Eur. J.* **1998**, *4*, No. 5

rhodium complex and the manganese porphyrins into the different bilayer systems, closed vesicles were still present. The diameters (3000–5000 Å) of these vesicles were the same as those without rhodium complex and manganese porphyrin. These results are in agreement with earlier findings that **Rh-5** and **Mn-2** can be incorporated into polymerized positively charged bilayers.[11] DPPC vesicles containing **Rh-5** were also prepared in aqueous solutions of riboflavin (**RF**), methylviologen (**MV**$^{2+}$), and **Mn-4** (see Experimental Section). Electron micrographs showed that in these cases vesicles were also still present.

Differential scanning calorimetry (DSC) measurements revealed that the phase-transition temperature of the DPPC vesicles ($T_c = 38\,^\circ$C)[12] was not influenced by incorporation of **Rh-5** and **Mn-1** (vide infra).

Electrochemistry: The reduction potential of membrane components often depends on the vesicle charge. The reduction potential of vesicle-bound viologens, for example, increases upon going from negatively charged DHP vesicles to positively charged vesicles.[13] In our case stabilization of the rhodium(III) species by the anionic DHP head groups and destabilization by the cationic DODAC head groups can be expected. Our earlier studies on polymerized aggregates showed that the reduction potential of the rhodium complex also depends on its location in positively charged bilayers.[11] Since the kinetics of the reduction of **Rh-5**, the first step in the catalytic epoxidation process, can be influenced by the reduction potential of this complex, electrochemical experiments were performed. Cyclic voltammograms (CV) of **Rh-5** incorporated in bilayers of DODAC, DPPC, or DHP were recorded at neutral pH. The results are listed in Table 1.

Table 1. Kinetic parameters determined from Equation (6)[a] and electrochemical data of **Rh-5** in different types of vesicles.[b]

Lipid	k_{max} [nmol L^{-1}s^{-1}]	K_M [M]	$E_{1/2}$ [V][c]	ΔE_p [mV]	i_b/i_f
DODAC	220	0.030	-0.92	96	0.8
DPPC	30	0.071	-0.92	104	0.8
DHP	150	0.035	-[d]	-	-

[a] $T = 49\,^\circ$C in the case of DODAC and DPPC vesicles, $T = 74\,^\circ$C in the case of DHP vesicles. [b] **Rh-5** in water $E_{1/2} = -0.90$ V, $\Delta E_p = 80$ mV, and $i_b/i_f = 0.8$. [c] Conditions: [surfactant] = 926 μM, [**Rh-5**] = 72 μM, pH = 7.0 (buffer of ethylmorpholine (50 mM)), $T = 25\,^\circ$C. [d] No redox waves were observed.

In DODAC and DPPC vesicles, clear reduction and oxidation waves were observed. When the vesicle solution in the cell was replaced by the buffer solution (pH 7), reduction and oxidation waves were still observed, indicating strong adsorption of the electroactive component on the electrode. The peak currents varied with the scan rate up to 500 mV s^{-1}; this is characteristic of the presence of adsorbed electroactive species on the electrode.[14]

According to cyclic voltammetry the reduction potential of **Rh-5** is the same in DODAC and DPPC bilayers, and very similar to that of **Rh-5** in H_2O (Table 1; **Rh-5** in water: $E_{1/2} = -0.90$ V, **Rh-5** in DODAC and DPPC bilayers: $E_{1/2} = -0.92$ V). This similarity may be due to strong adsorption of **Rh-5** and the surfactants on the electrode.[15] Cluster formation of **Rh-5** in these types of bilayers may also play a role; however, this cannot explain the observations made in the chemical reduction of **Rh-5** (vide infra).[16] It is also possible, but unlikely, that the head groups of the different surfactants have no effect on the reduction potential.[13] The reduction potential of **Rh-5** in the DODAC aggregates was shifted by 60 mV to more negative potential relative to **Rh-5** incorporated in polymerized DODAC aggregates ($E_{1/2} = -0.86$ V versus ferrocenecarboxylic acid).[11] This difference may arise because the rhodium complex is located at different positions in the respective bilayers. It may also be due to the fact that in the present experiments a different **Rh-5**/surfactant ratio was used. In the case of the negatively charged DHP bilayers no electrochemical reduction of **Rh-5** was observed (Table 1). This may be the result of electrostatic repulsion between the DHP head groups and the cathode. The electron transfer process between the vesicle-bound rhodium complexes and the electrode may become too slow in this case.[17]

Chemical reduction of Rh-5: The reduction of **Rh-5** by formate was investigated in various vesicles under an argon atmosphere. The formation of the Rh^{I} species ($\lambda_{max} = 520$ nm) was monitored by UV/Vis spectroscopy, and the resulting progress curves were fitted under the assumption of first-order kinetics. The results are listed in Table 2.

Table 2. Rate constants for the reduction of bilayer-anchored **Rh-5** by formate and experimentally determined pK_a^{obs} values of (**Rh-5**)-H$^+$ in different types of amphiphiles.[a]

Entry	Surfactant	T [°C]	pK_a^{obs}	k_1 [ms^{-1}]	pH[c]
1	DHP	72	8.6	10	10.5
2	DPPA	72	9.1	1.6	10.2
3	DPPA/DPPC[b]	64	7.6	2.5	9.4
4	DPPC	47	5.7	3.2	7.0
5	DODAC	47	4.9	13	5.9
6	DODAC	72	5.0	25	5.9

[a] Conditions: [surfactant] = 926 μM, [**Rh-5**] = 72 μM. [b] Molar ratio = 1. [c] pH at which the rate constant for reduction of bilayer-anchored **Rh-5** was measured.

The reduction of **Rh-5** by formate in vesicles of different types of amphiphiles is fastest in positively charged bilayers and slowest in negatively charged bilayers. In all cases an increase in temperature leads to an increase in reduction rate. The proposed mechanism for the reduction of **Rh-5** is given in Equations (2)–(4).[18] Decomposition of the Rh^{III} formate

$$[Rh^{III}Cl]^+ + HCOO^- \rightleftharpoons [Rh^{III}HCOO]^+ + Cl^- \quad (2)$$

$$[Rh^{III}HCOO]^+ \rightarrow [Rh^{III}H]^+ + CO_2 \quad (3)$$

$$[Rh^{III}H]^+ \rightleftharpoons [Rh^{I}] + H^+ \quad (4)$$

complex to give an Rh^{III} hydride and carbon dioxide [Eq. (3)] is thought to be the rate-determining step.[18] The pH

conditions for the reduction experiments (vide infra) were chosen such that only Rh^{I} is formed [Eq. (4); see Table 2]. The rate of reduction of Rh^{III} mainly depends on the concentration and on the relative stability of the Rh formate complex cation. Although the electrochemical results (vide supra) were not conclusive, the Rh^{III} formate species is expected to be stabilized in a negatively charged membrane matrix, and this should lower the reduction potential. Thus the lowest reduction rate is expected to occur with DHP and DPPA. The concentration of Rh formate is highest at the surface of the positively charged DODAC bilayers because the concentration of formate at the surface of this aggregate is relatively high. These effects may account for the observed increase in the first-order rate constants in the series DPPA < DPPA/DPPC < DPPC < DODAC (Table 2). The relatively high rate of reduction found in DHP bilayers compared with DPPA bilayers, which are also negatively charged, is remarkable. In general the relative stability of the Rh formate complex also depends on its location in the bilayer, which may be different in the two types of bilayer.[11]

The Rh^{I} species is only generated above a certain pH value.[19] The reduction of rhodium(III) by formate initially gives a rhodium(III) hydride species [Eq. (3)], which is formed by hydride transfer from the formate anion to the rhodium(III) center. The Rh^{III} hydride can decompose, depending on the pH, into a rhodium(I) species [Eq. (4)].[11] The pK_a of the Rh^{III} hydride complex can give information about the local concentration of protons [necessary for the epoxidation reaction, Eq. (1)] at the bilayer/water interface. The acidity of the membrane-bound rhodium species depends on the bilayer surface potential, which is determined by the type of amphiphile. The relation between the intrinsic pK_a^i and the observed pK_a^{obs} is given by Equation (a),[20] where $\Psi(x)$ is the surface potential, R the gas constant, F the Faraday constant, and T the temperature. The intrinsic pK_a^i is the pK_a in the

$$pK_a^{obs} = pK_a^i - F\Psi(x)/2.303\,RT \qquad (a)$$

absence of any surface potential. Its value depends only on the relative stabilities of the rhodium species involved in Equation (2).[21] For our rhodium complex this pK_a^i value is roughly 7.5.[11] The pK_a^{obs} of the Rh^{III}–H complex can be determined by measuring the $[Rh^{I}]/[Rh]_{total}$ ratio as a function of pH (Figure 3). The experimental curves were fitted by assuming a single acid–base dissociation equilibrium, and the resulting pK_a^{obs} values are listed in Table 2.

It can be seen from Figure 3 that the type of amphiphile has a large effect on the pK_a^{obs} of the bilayer-anchored rhodium complex. The value of pK_a^{obs} increases in the series DODAC < DPPC < DPPC/DPPA < DHP < DPPA. This order can be explained in terms of the effect of the surface potential of the bilayer on the proton concentration. In the case of the DODAC bilayers, the concentration of protons at the bilayer surface will be relatively low due to electrostatic repulsion with the positively charged DODAC head groups. This gives rise to a relatively high degree of dissociation of the membrane-bound rhodium hydride complex. In the series from DODAC to DPPA, the charge of the vesicles changes from positive through zwitterionic to negative. This results in an increasing proton concentration at the vesicle surface and hence a higher pK_a^{obs}.

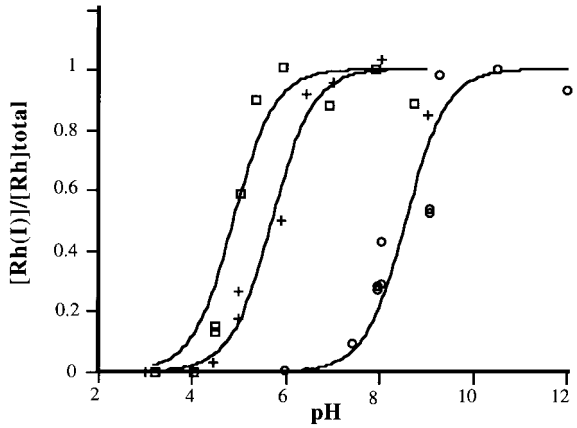

Figure 3. Fraction of the Rh^{I} complex as a function of pH for **Rh-5** anchored to DODAC (□), DPPC (+), and DHP (○) vesicles. Conditions: [surfactant] = 926 μM, [**Rh-5**] = 72 μM.

Reduction of electron carriers: Methylviologen ($\mathbf{MV}^{2+}$), and riboflavin (**RF**) are often used as electron carriers in redox reactions.[22, 23] This prompted us to investigate whether these compounds can act as mediators between the rhodium complex and the manganese porphyrin. Carrier-mediated electron transfer is one of the crucial steps in the reductive activation of molecular oxygen by cytochrome P450. First we investigated whether methylviologen and riboflavin can be reduced by **Rh-5** incorporated in DPPC vesicles under an argon atmosphere.

When **Rh-5** in DPPC was added to a methylviologen solution, the solution turned dark blue, indicating that the $\mathbf{MV}^{+}$ radical was formed.[24] The UV/Vis spectrum showed a sharp band at 394 nm and a broad band at 602 nm, characteristic of $\mathbf{MV}^{+}$. After the complete disappearance of $\mathbf{MV}^{2+}$, the UV/Vis spectrum remained unchanged and no precipitation occurred indicating that no $\mathbf{MV}^{0}$ or radical dimers were formed. The potential for the reduction step of $\mathbf{MV}^{+}$ is about −0.90 V versus SCE in the presence of zwitterionic bilayers.[13] The two-electron reduction potential of our rhodium complex is −0.62 V versus SCE, so it is not surprising that the reduction of $\mathbf{MV}^{2+}$ stops after the first single-electron reduction step. The reduction progress curve of $\mathbf{MV}^{2+}$ showed zero-order kinetics, and the reaction rate was 219 nmol L^{-1} s^{-1} at 71 °C. The percentage m of monomer $\mathbf{MV}^{+}$ with respect to the radical dimer $(\mathbf{MV}^{+})_2$ can be calculated from the optical spectrum by Equation (b).[13] The absorbance at 552 nm (A_{552}) corresponds to the monomer–dimer isosbestic point. In our case the monomer content amounted to more than 90%.

$$m = 100(A_{602}/A_{552} - 0.59)/0.98 \qquad (b)$$

The reduction of riboflavin (**RF**) was also catalyzed by **Rh-5** incorporated in DPPC vesicles. The reduction followed zero-order kinetics. The reduction rate was measured at different temperatures, and the activation energy was calculated from

0947-6539/98/0405-0874 $ 17.50+.50/0 *Chem. Eur. J.* **1998**, *4*, No. 5

the slope of the Arrhenius plot as $E_a = 80\ kJ\,mol^{-1}$. This activation energy is in the same range as that reported for the reduction of nicotinamides with [RhCp*(bipy)Cl_2] as catalyst ($E_a = 88\ kJ\,mol^{-1}$) but is lower than that found for the reduction of flavin in the presence of rhodium complexes covalently anchored to positively charged bilayers.[11] The reduction rate of **RF** in DPPC vesicles at 70 °C as calculated from the Arrhenius plot is about $k_0 = 100\ nmol\,L^{-1}\,s^{-1}$, which is about two times slower than the reduction rate of $\mathbf{MV}^{2+}$ at this temperature ($T = 71$ °C, $k_0 = 219\ nmol\,L^{-1}\,s^{-1}$). This difference is probably the result of the different stoichiometries of the reduction reactions of **RF** and $\mathbf{MV}^{2+}$ by **Rh-5**, which are two-electron reduction [Eqs. (5)–(8)] and one-electron reduction [Eqs. (9)–(12)] reactions, respectively.[11]

$$[Rh^{III}H]^+ + RF \rightarrow [Rh^{III}]^{2+} + RF\text{-}H^- \quad (5)$$

$$[Rh^{I}] + RF \rightarrow [Rh^{III}]^{2+} + RF^{2-} \quad (6)$$

$$RF^{2-} + H^+ \rightleftharpoons RF\text{-}H^- \quad (7)$$

$$RF\text{-}H^- + H^+ \rightleftharpoons RF\text{-}H_2 \quad (8)$$

$$[Rh^{III}H]^+ + MV^{2+} \rightarrow [Rh^{II}]^+ + H^+ + MV^+ \quad (9)$$

$$[Rh^{I}] + MV^{2+} \rightarrow [Rh^{II}]^+ + MV^+ \quad (10)$$

$$[Rh^{II}]^+ + MV^{2+} \rightarrow [Rh^{III}]^{2+} + MV^+ \quad (11)$$

$$2[Rh^{II}]^+ \rightleftharpoons [Rh^{I}] + [Rh^{III}]^{2+} \quad (12)$$

The electron carriers can be reduced by both $[Rh^{III}H]^+$ and $[Rh^{I}]$ complexes [see also Eq. (4)]. Which reaction occurs depends on the pH and on the reaction constants in Equations (5) and (6) and (9) and (10), respectively. The reduction of $\mathbf{MV}^{2+}$ may lead to the formation of a Rh^{II} species [Eqs. (9) and (10)], which rapidly disproportionates ($k = 10^9\ M^{-1}\,s^{-1}$) into the Rh^{I} and Rh^{III} complexes [Eq. (12)].[11] Another possibility is that the Rh^{II} reacts with another $\mathbf{MV}^{2+}$ [Eq. (11)]. The reduction of both electron carriers is zero order with respect to carrier, which indicates again that the formation of the rhodium hydride complex is the rate-determining step. This rhodium hydride complex reduces two equivalents of paraquat but only one equivalent of riboflavin.

Reduction of manganese porphyrins: First we investigated the intervesicular reduction of manganese porphyrins (Figure 4) under an argon atmosphere in the presence and absence of an electron carrier. For this process, **Rh-5** and manganese porphyrin were incorporated in separate vesicles of DPPC and DHP. In all cases reduction of the manganese porphyrin took place after a short induction period (vide infra) in a zero-order reaction. The results are listed in Table 3 (entries 1–5). The intervesicular reduction of manganese porphyrins proceeds both with and without electron carriers (Table 3, entries 1, 2, and 5 vs. 3 and 4). Thus the rhodium-containing vesicles can directly reduce the porphyrin-containing vesicles. An explanation for this may be that vesicle fusion takes place under the conditions of our experiments. Addition of $CaCl_2$ to induce vesicle fusion, however, did not enhance the reduction rate.[25] The intervesicular reduction is accelerated by the addition of riboflavin (**RF**) or methylviologen ($\mathbf{MV}^{2+}$) (Table 3, entries 3, 4 vs. 2), indicating that these electron carriers shuttle between the rhodium- and manganese-containing vesicles. In the natural cytochrome P450 system, the flavin-containing reductase shuttles between the NADPH cofactor and the cytochrome P450 catalyst.[1]

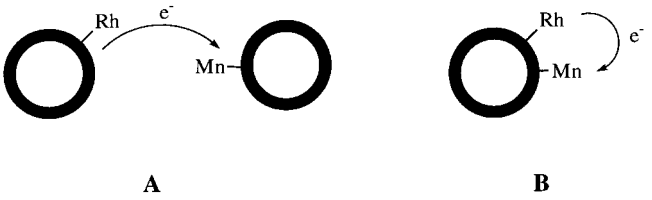

Figure 4. Schematic representation of the intervesicular (A) and intravesicular (B) reduction of Mn^{III} porphyrin with **Rh-5** as catalyst.

Table 3. Rate constants for the reduction of various manganese porphyrins in different type of amphiphiles catalyzed by **Rh-5** under argon atmosphere.[a]

Entry	Surfactant	Reaction type	T [°C]	Porphyrin	k_0 [$nmol\,L^{-1}s^{-1}$]
1[b]	DPPC	intervesicular	48	**Mn-1**	3.3
2[c]	DPPC	intervesicular	48	**Mn-2**	5.1
3[d]	DPPC + RF	intervesicular	48	**Mn-2**	9.2
4[e]	DPPC + MV^{2+}	intervesicular	48	**Mn-2**	11.1
5[f]	DHP	intervesicular	75	**Mn-1**	3.7
6[f]	DHP	intervesicular	75	**Mn-1**	60
7[c]	DPPC	intervesicular	48	**Mn-1**	12.4
8[c]	DPPC	intervesicular	48	**Mn-2**	12.6
9[c]	DPPC	intravesicular	48	**Mn-3**	9.4
10[c]	DPPC	intravesicular	48	**Mn-4**	12.5
11[b]	DODAC	intravesicular	75	**Mn-1**	> 100
12[b]	DHP	intravesicular	75	**Mn-1**	20.0

[a] For reaction conditions, see Experimental Section. [b] Conditions: [surfactant] = 926 μM, [**Mn**] = 2.4 μM, [**Rh-5**] = 2.4 μM. [c] Conditions: [surfactant] = 926 μM, [**Mn**] = 4.8 μM, [**Rh-5**] = 6.7 μM. [d] **RF** = riboflavin. Conditions: [surfactant] = 926 μM, [**Mn**] = 4.8 μM, [**Rh-5**] = 6.7 μM, [**RF**] = 10 μM. [e] $\mathbf{MV}^{2+}$ = methylviologen. Conditions: [surfactant] = 926 μM, [**Mn**] = 4.8 μM, [**Rh-5**] = 6.7 μM, [$\mathbf{MV}^{2+}$] = 10.5 μM. [f] Conditions: [surfactant] = 960 μM, [**Mn**] = 2.4 μM, [**Rh-5**] = 12 μM.

As the intervesicular reduction of manganese(III) porphyrins also took place without electron carriers, we investigated the intravesicular reduction (Figure 4) of this catalyst in the absence of carriers. The reactions were zero order. The influence of the type of membrane on the reduction rate of **Mn-1** is given in Table 3, entries 7, 11, and 12. The rate depends on the charge of the surfactant used. At the same temperature and the same **Rh-5**/**Mn-1** ratio the rate is higher for DODAC vesicles than for DHP vesicles. Since the formation of the rhodium hydride complex is the rate-determining step in the reduction of the manganese(III) porphyrin, we propose the same explanation for the observation that the reaction is zero order as for the reduction of Rh^{III} in the different types of surfactants (vide supra, Table 2), which is also zero order.

The influence of the location of the porphyrin in the vesicle bilayer on the rate of its reduction by formate and **Rh-5** was studied in DPPC vesicles. We have shown that the reduced porphyrins **Mn-1** and **Mn-2** are located in the center of the bilayer, whereas **Mn-3** is located at the bilayer surface.[26] The porphyrin **Mn-4** will be located in the water phase.[20] After a short induction period all porphyrins were reduced in zero-order reactions by **Rh-5**. The results are listed in Table 3 (entries 7–10); the reduction rates of manganese(III) porphyrins **Mn-1** to **Mn-4** are roughly equal. The overall concentrations of the porphyrins used in our experiments are identical, but the local concentrations will differ. For example, in the case of **Mn-3**, which is located at the bilayer interface, the concentration of a porphyrin in the neighborhood of the rhodium complex will be higher than in the case of **Mn-4** which is dissolved in the aqueous phase. The fact that the reduction rate of the manganese porphyrins is independent of the location and concentration of these molecules indicates that the rate-determining step of this reaction is the decomposition of the Rh formate complex into Rh^{III} hydride and carbon dioxide.[27]

The reduction rate of **Mn-1** in DPPC and DHP vesicles was also measured as a function of the [**Rh-5**]/[**Mn-1**] ratio. A linear relation was found, with the same slope for both vesicle systems (Figure 5). A similar relationship between the rate of reduction and the rhodium/substrate ratio was observed for the reduction of flavin.[11]

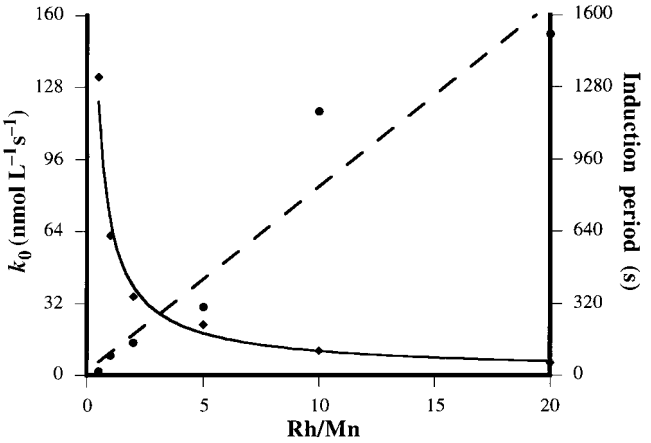

Figure 5. Induction period (◆) and reduction rate of **Mn-1** (●) as a function of the [**Rh-5**]/[**Mn-1**] ratio in DPPC vesicles. Conditions: [DPPC] = 926 μM, [**Mn-1**] = 2.4 μM, [**Rh-5**] = 2.4 n μM (n = **Rh-5/Mn-1**); pH 7.0; T = 48 °C.

The induction period for the reduction of **Mn-1** in DPPC vesicles was measured as a function of the concentration of the **Rh-5** catalyst. *The induction period* was found to be inversely proportional to the [**Rh-5**]/[**Mn-1**] ratio. One possible explanation is that a certain amount of oxygen is present when the solution is prepared and reacts first with the manganese(II) species. At a higher concentration of **Rh-5** the manganese(II) porphyrin is formed faster, and the amount of reduced porphyrin that can initially react with oxygen is higher. This will result in a shorter induction period because only when all the oxygen has reacted can the net reduction of **Mn-1** take place.

The reduction of **Mn-1** in DPPC vesicles was measured as a function of temperature. No inflection point in the rate versus temperature plot was observed at the phase-transition temperature of the vesicle bilayers (42 °C) and a linear relation between the reduction rate and $1/T$ was found. The activation energy, calculated from the slope of this Arrhenius plot, was $E_a = 87 \pm 5$ J mol^{-1}.

Reduction experiments in DPPC vesicles were also carried out in air. At 48 °C and a formate concentration of 0.25 M, no reduction of Mn^{III} porphyrin was observed at [Rh]/[Mn] ratios less than 10. At [Rh]/[Mn] ratios higher than 10, however, reduction took place. Oscillations in the concentration of manganese(II) porphyrin were detected at a [Rh]/[Mn] ratio of 10.[10b] After an induction period of about 30 min, the manganese(II) porphyrin was gradually formed, and about 50 min after the start of the experiment, the onset of oscillations with a periodicity of about 90 s was observed. When the Mn^{III} species was monitored, the complementary progress curve was obtained.

The oxygen concentration in solution was measured with a semibatch reactor containing an oxygen-selective Clark electrode.[28] The oxygen concentration was 5.2 mg L^{-1} at the start of the experiment and dropped to almost zero when the manganese(II) species started to form. When an oxygen/nitrogen gas stream with 0.1 % oxygen was used, no oscillation was observed and a linear increase in Mn^{II} concentration was seen. When this species had reached its maximum, a bathochromic shift of 5 nm for the B and Q bands was detected by UV/Vis spectroscopy. Changes in temperature caused the oscillations to cease.

In air no net reduction is observed at [**Rh-5**]/[**Mn-1**] < 10; this indicates that the reoxidation of the manganese(II) porphyrin by molecular oxygen is considerably faster than its reduction. At [**Rh-5**]/[**Mn-1**] ratios greater than 10, the situation is reversed and a net reduction of **Mn-1** occurs. At [**Rh-5**]/[**Mn-1**] = 10 apparently an oscillating reaction takes place in which the manganese porphyrin shuttles between the +2 and +3 states. The two-dimensional projection of the phase plot of the manganese(II) porphyrin is shown in Figure 6.[28] This so-called attractor reveals that the reaction

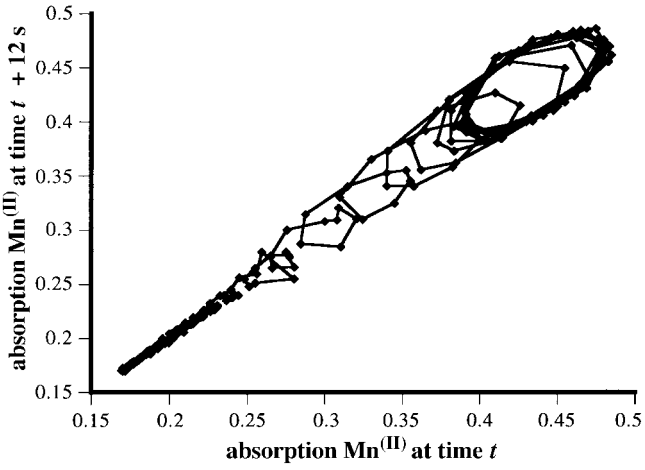

Figure 6. Oscillating reduction of **Mn-1** by **Rh-5** and formate in air at 48 °C. The change in absorption at 435 nm (Mn^{II}) was measured as a function of time and plotted as described in ref. [28]. Conditions: [DPPC] = 926 μM, [**Mn-1**] = 2.4 μM, [**Rh-5**] = 22 μM; pH 7.0.

0947-6539/98/0405-0876 $ 17.50+.50/0 *Chem. Eur. J.* **1998**, *4*, No. 5

has an elliptical periodic oscillation in the absorption range 0.4–0.5. This behavior suggests that whatever the initial concentration of Mn^{II} is, the system settles into the same periodic variation of concentration (ellipse). Small changes in temperature prohibited the oscillation, and this is consistent with the fact that both the reduction and oxidation reactions are strongly temperature dependent (vide supra). The bathochromic shift of 5 nm observed for the B and Q bands of the manganese(II) porphyrin might indicate that the porphyrin molecules temporarily move to a part of the bilayer which has a lower polarity and is free of solvent molecules that can coordinate to the axial position, that is, move away from the bilayer/water interface.[26, 29] Calculations and further experiments are in progress to elucidate the cause of the oscillatory behavior.

Formate concentration dependence: The dependence of the rate of reduction of **Mn-1** on the formate concentration was investigated in different types of vesicles. In the case of DHP vesicles the reaction temperature was 74 °C, and for DPPC and DODAC vesicles 49 °C, which is above the phase-transition temperature of the vesicle bilayers. The experimental curves could be approximately fitted by using Michaelis–Menten type kinetics [Eqs. (c) and (d)],[11, 18]

$$k_0 = \frac{k_{max}[HCOO^-]}{[HCOO^-] + K_M} \quad (c)$$

$$K_M = K_b' e^{-\frac{F\Psi(x)}{RT}} \quad (d)$$

where k_{max} is the maximal reduction constant and K_M is a constant related to the binding constant of formate to the rhodium complex K_b' and the surface potential of the bilayer at the site of the rhodium complex $\Psi(x)$. The calculated values for K_M and k_{max} are listed in Table 1.

The fact that Michaelis–Menten type kinetics are found for the reduction of the manganese(III) porphyrins at different formate concentrations indicates that the coordination of formate to the rhodium center takes place in an equilibrium reaction that precedes the rate-determining step, which is the formation of the rhodium(III) hydride species.[18] The latter reacts rapidly with the manganese(III) porphyrin.

The values of k_{max} and K_M (Table 1) for DHP are difficult to compare with those for DPPC and DODAC because they had to be obtained at different temperatures. The k_{max} appears to be higher in DODAC bilayers than in DPPC bilayers (Table 1). The rate constant for the reduction of **Mn-1** will be dependent on the rate of decomposition of the rhodium formate complex into the rhodium(III) hydride complex. It is conceivable that the rhodium formate complex is less stabilized in the positively charged DODAC vesicles than in the negatively charged DPPC bilayers, and this may result in a lower activation energy and a higher reaction rate for the decomposition reaction.

Epoxidation experiments: **Mn-1** was chosen as the catalyst in the epoxidation experiments because it displays almost no aggregation in vesicle bilayers, and its reduced form has been shown to be located in the hydrophobic part of the membrane (Figure 2).[26] The epoxidation of various substrates with molecular oxygen in the presence of **Rh-5** and **Mn-1** as catalysts was investigated in different types of vesicles. The results are listed in Table 4.

Table 4. Epoxidation of alkenes by the membrane-bound cytochrome P450 mimic.[a]

Entry	Surfactant	Substrate	Product[b]	T.O.[c]
1	DHP	α-pinene	α-pinene oxide	360
2	DPPC[d]	α-pinene	α-pinene oxide	16
3	DHP	*cis*-stilbene	*cis*-stilbene oxide	45
4	DHP	limonene	limonene oxide	50
5	DHP	styrene	styrene oxide	55
6	DHP[e]	styrene	styrene oxide	5
7	DODAC	styrene	styrene oxide	0
8	DODAC[e]	styrene	styrene oxide	0
9	DPPC[d]	styrene	styrene oxide	4
10	DHP	ethylbenzene	acetophenone	400

[a] [**Mn-1**] = 2.4 μM, [**Rh-5**] = 2.4 μM, for further reaction conditions see Experimental Section. The reaction was monitored by GLC for 1 h. No destruction of the catalyst was found after that period. [b] No oxidation was observed without vesicles or when any of the components of the catalytic system were omitted, except in the case of ethylbenzene. Here also some oxidation took place when **Rh-5** was omitted. [c] T. O. = turnover number: [epoxide]/[**Mn-1**] per h, calculated from the initial part of the conversion/time plot. [d] **Rh-5**/**Mn-1** molar ratio = 5. [e] **Rh-5**/**Mn-1** molar ratio = 10.

All substrates tested were epoxidized by the catalytic systems based on DHP and DPPC vesicles. The turnover numbers (Table 4) are higher than those obtained with the two-phase system.[9] They are in the same range as those observed for the natural system (1 nmol product per nmol P450* per min).[1] The effect of the membrane environment on the catalytic epoxidation is more pronounced when the DHP vesicles are replaced by the DODAC vesicles. In the latter membrane system, no epoxidation of alkenes was observed (Table 4, entries 7 and 8). Presumably, the concentration of protons is too low for the catalytically active Mn^V oxo species[2] to be formed at the positively charged interface. When the [Rh]/[Mn] ratio was increased from 1 to 10, the turnover number of the reaction decreased considerably (Table 4, entry 6). This may be due to the fact that more electrons become available because of the higher concentration of rhodium centers. As a result a side reaction can take place that produces water (the so-called nonproductive pathway, Figure 1).[2] The turnover numbers for DPPC vesicles are much lower than those for the DHP vesicles. This behavior is probably not the result of the lower temperature, because in the case of DPPC a higher concentration of rhodium was used, which makes the reduction rates of **Mn-1** in the two systems almost equal (DHP: $T = 75\,^\circ C$, [**Rh-5**]/[**Mn-1**] = 1, $k_0 = 20\ nmol\,L^{-1}\,s^{-1}$; DPPC: $T = 47\,^\circ C$, [**Rh-5**]/[**Mn-1**] = 5, $k_0 = 30\ nmol\,L^{-1}\,s^{-1}$). The oxygen concentration will be higher for DPPC vesicles at 47 °C than for DHP vesicles at 75 °C, which should be an advantage for the former system. A reasonable explanation for the observed difference in turnover numbers is that the concentration of protons at the DPPC surface is too low, as in the case of DODAC vesicles. The pK_a^{obs} value of 5.7 (Table 2) for DPPC is closer to that of DODAC ($pK_a^{obs} = 5.0$) than to that of DHP ($pK_a^{obs} = 8.6$).

UV/Vis spectroscopy showed that the porphyrin catalyst did not decompose during the oxidation reactions (< 5% decomposition after 1 h). This remarkably high stability, which is in contrast with the two-phase system previously reported, is thought to be the result of the stabilizing effect of the bilayers.[9]

The reaction product α-pinene oxide was converted (> 90%) into other products within a period of one hour (vide infra). Limonene oxide decomposed (50%) into unidentified products. The turnover numbers in Table 4 are not corrected for this decomposition reaction. Styrene oxide and stilbene oxide were stable under the experimental conditions. The epoxidation of styrene was measured at **Rh-5**/**Mn-1** ratios of 1 and 10. In both cases phenylacetaldehyde was also detected as a reaction product (10% with respect to styrene epoxide). In the case of *cis*-stilbene no *trans*-stilbene epoxide was formed; this may indicate a concerted reaction between the Mn^{V} oxo species and the alkene.[30] Ethylbenzene was oxidized to acetophenone. In this case the oxidation reaction also occurred when **Rh-5** was omitted. Acetophenone was not formed, however, when **Mn-1** was absent. It is known that ethylbenzene can undergo autooxidation in air.[31] In our case the manganese porphyrin presumably serves as an initiator for this autocatalytic reaction.

α-Pinene oxide stability: The stability of α-pinene oxide under the reaction conditions was investigated by mixing it with DHP and DPPC vesicles. Identical decomposition curves of the epoxide were found for vesicles with and without catalyst. The $t_{1/2}$ values for decomposition of α-pinene oxide in the presence of DHP at 75 °C and DPPC at 47 °C were 2 and 7 min, respectively. Four main products were formed in the decomposition reaction, as shown by GC–MS: campholenic aldehyde, *trans*-carveol, pinocamphone, and *trans*-sobrerol (Figure 7). These are the normal isomerization products of α-pinene oxide and are the result of an acid-catalyzed ring opening reaction.[32]

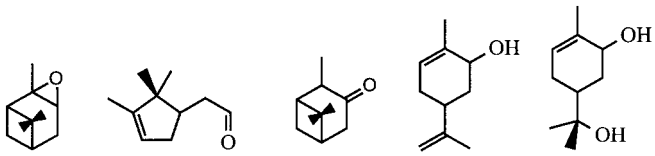

A B C D E

Figure 7. α-Pinene oxide (A) and its decomposition products campholenic aldehyde (B), pinocamphone (C), *trans*-carveol (D), and *trans*-sobrerol (E).

Conclusions

A supramolecular cytochrome P450 mimic that incorporates all features of the natural system, namely, 1) a membrane-bound metalloporphyrin, 2) an axial ligand (*N*-methylimidazole), 3) an electron donor (rhodium complex/formate), 4) molecular oxygen as oxygen donor, and 5) a membrane system that holds the components within its bilayer, has been developed. The reduction rate of the rhodium complex incorporated in closed bilayers (vesicles) of surfactants with positive, zwitterionic, or negative head groups is highly dependent upon the vesicle charge. The reduced rhodium complex efficiently catalyzes the reduction of methylviologen, riboflavin, and various manganese(III) porphyrins. The charges of the surfactant head groups determine the degree of dissociation of the reduced Rh^{III} hydride complex into Rh^{I} and a proton, as well as the reduction rate of the manganese(III) porphyrins, which increases on going from negatively to positively charged surfactants. Under aerobic conditions net reduction of Mn^{III} porphyrins takes place when the concentration of rhodium is more than 10 times that of the porphyrin. At a [Rh]/[Mn] ratio of 10, the concentration of Mn^{II} porphyrin oscillates. A variety of substrates has been epoxidized with the cytochrome P450 model system with turnover numbers on the same order of magnitude as those of the natural system. The charge on the vesicles has a dramatic effect on the catalytic epoxidation activity of the mimic. In the case of the positively charged DODAC vesicles no epoxidation of alkenes was observed, presumably because the concentration of protons is too low to allow formation of the catalytically active Mn^{V} oxo species.

Experimental Section

Instrumentation: Infrared and UV/Vis spectra were recorded with Perkin-Elmer 298 and Perkin-Elmer Lambda 5 spectrophotometers, respectively. Differential scanning calorimetry measurements were performed on a Perkin-Elmer DSC 7 instrument. Electrochemical measurements were carried out with a PAR 175 potentiostat. Transmission electron microscopy was performed on a Philips EM 201 microscope. FAB mass spectra were recorded on a VG 7070E instrument with *m*-nitrobenzyl alcohol as the matrix. GC analyses were carried out with a Varian 3700GC instrument containing a Chrompack column (WCOT/CP-SIL5CB, diameter = 0.25 μm). The injection post temperature and the FID detector temperature in all cases were 250 °C and 260 °C, respectively. A specific temperature program was used for each substrate.

Materials: For the preparation of the vesicles absolute ethanol, distilled tetrahydrofuran, and deionized water were used. *N*,*N*-Dioctadecyl-*N*,*N*-dimethylammonium chloride (DODAC) was prepared from *N*,*N*-dioctadecyl-*N*,*N*-dimethylammonium bromide (DODAB) by ion-exchange chromatography.[11] L-α-Dipalmitoylphosphatidylcholine (DPPC), dihexadecyl phosphate (DHP), L-α-dipalmitoylphosphatidic acid (DPPA), and methyl tosylate were purchased from Sigma. Thin-layer chromatography (TLC) was performed on precoated F-254 plates (Merck). Column chromatography was carried out on basic alumina or Silica 60H (Merck). *N*-(2-(2-(2,2′-Bipyridyl-5-carbosamido)-ethoxyethyl)-*N*,*N*-dihexadecyl-*N*-methylammonium)pentamethylcyclopentadienylrhodium trichloride (**Rh-5**) was a gift of Dr J. H. van Esch.[11] 21*H*,23*H*-5,10,15,20-Tetra(2,6-dichlorophenyl)-porphyrin,[33] 21*H*,23*H*-5,10,15,20-tetra(4-hexadecyloxyphenyl)porphyrin, 21*H*,23*H*-5,10-di(4-pyridyl)-15,20-di(4-hexadecyloxyphenyl)porphyrin, and 21*H*,23*H*-5,10,15,20-tetra(4-pyridyl)porphyrin were prepared according to literature procedures.[11, 34]

5,10,15,20-Tetra(2,6-dichlorophenyl)porphyrin manganese(III) acetate (**Mn-1**) was synthesized by the literature method[35] from 21*H*,23*H*-5,10,15,20-tetra(2,6-dichlorophenyl)porphyrin (50 mg) and manganese(III) acetate (300 mg). Yield: 40 mg (72%) of **Mn-1** as a green powder. R_f (MeOH/EtOAc, 1/1, v/v) = 0.7. FAB-MS: m/z: 943 [$M - CH_3COO^-$]. UV/Vis ($CHCl_3$): λ_{max} ($\lg \varepsilon$): 372 (4.50), 394 (4.34), 477 (4.77), 578 nm (3.85).

5,10,15,20-Tetra(4-hexadecyloxyphenyl)porphyrin manganese(III) chloride (**Mn-2**): A solution containing 21*H*,23*H*-5,10,15,20-(4-hexadecyloxyphenyl)porphyrin (50 mg), $NaHCO_3$ (100 mg) and manganese(II) chloride (150 mg) in THF (15 mL) was heated to reflux with stirring under nitrogen for 24 h. The solvent was evaporated under reduced pressure, and the product was purified by column chromatography on silica (MeOH/$CHCl_3$,

0947-6539/98/0405-0878 $ 17.50+.50/0 *Chem. Eur. J.* **1998**, *4*, No. 5

1/18, v/v). Yield: 45 mg (85%) of **Mn-2** as a green powder. R_f (MeOH/$CHCl_3$, 1/9, v/v) = 0.7. FAB-MS: *m/z*: 1629 [*M*]. UV/Vis ($CHCl_3$): λ_{max} (lg ε): 382 (4.60), 406 (4.56), 480 (4.87), 584 (3.83), 625 nm (4.00).

5,10-Di(4-pyridyl)-15,20-di(4-hexadecyloxyphenyl)porphyrin manganese(III) acetate was synthesized as described in the literature[35] from 21*H*,23*H*-5,10-di(4-pyridyl)-15,20-di(4-hexadecyloxyphenyl)porphyrin (100 mg) and manganese(III) acetate (100 mg). Yield: 98 mg (94%) of compound as a green powder. R_f (MeOH/$CHCl_3$, 1/9, v/v) = 0.15. UV/Vis ($CHCl_3$): λ_{max}: 378, 403, 479, 581, 619 nm.

5,10-Di(4-(methylpyridinium)-15,20-di(4-hexadecyloxyphenyl)-porphyrin manganese(III) acetate ditosylate (Mn-3): Under a nitrogen atmosphere, 5,10-di(4-pyridyl)-15,20-di(4-hexadecyloxyphenyl)porphyrin manganese(III) acetate (50 mg) and methyl tosylate (300 mg) were dissolved in a mixture of toluene/acetonitrile (10 mL, 2/1, v/v). The reaction mixture was stirred at 80 °C for 16 h. After cooling to room temperature, the reaction mixture was poured over a glass filter covered with silica. After washing with acetone (50 mL) to remove excess methyl tosylate, **Mn-3** was isolated by elution with (MeOH/$CHCl_3$, 1/1, v/v). Yield: 40 mg (61%) of product as a dark green powder. R_f (MeOH/$CHCl_3$, 1/9, v/v) = 0.1. FAB-MS: *m/z*: 1180 [*M* − 2tos − acetate]. UV/Vis ($CHCl_3$): λ_{max} (lg ε): 380 (4.61), 404 (4.51), 476 (5.16), 580 (4.08), 620 nm (3.87).

5,10,15,20-Tetra(4-pyridyl)porphyrin manganese(III) acetate: The compound was synthesized as described in the literature,[36] starting from 21*H*,23*H*-5,10,15,20-tetra(4-pyridyl)porphyrin (50 mg) and manganese(III) acetate (300 mg). Yield: 72% of product as a green powder. R_f (MeOH/$CHCl_3$, 1/9, v/v) = 0.05. UV/Vis ($CHCl_3$): λ_{max}: 368, 396, 473, 581, 616 nm.

5,10,15,20-Tetra(4-(1-methylpyridinium))porphyrin manganese(III) pentachloride (Mn-4) was synthesized according to a literature procedure[36] from 5,10,15,20-tetra(4-pyridyl)porphyrin manganese(III) acetate (50 mg) and methyl tosylate (400 mg), and converted to the corresponding chloride salt by ion exchange chromatography. Yield: 52 mg (72%) of **Mn-4** as a dark green powder. FAB-MS: *m/z*: 766 [$M-4Cl^-$], 731 [$M-5Cl^-$]. UV/Vis (EtOH): λ_{max} (lg ε): 372 (4.12), 396 (4.05), 461 (4.55), 569 (3.57), 620 nm (3.87).

Vesicle preparation: Aliquots of stock solutions of manganese(III) porphyrin, **Rh-5**, and surfactant, calculated to give the desired concentrations, were mixed in a test tube. The solvent was evaporated under a stream of nitrogen to give a homogeneous thin film. This film was dissolved in ethanol/THF (100 μL, 1/2, v/v). Half of the solution was injected into an ethylmorpholine/formate buffer solution (5 mL) at a temperature above the phase-transition temperature of the surfactant bilayer: for DODAC T_c = 38 °C,[37] for DPPC T_c = 42 °C,[12] for DPPA T_c = 58 °C,[38] and for DHP T_c = 72 °C.[39]

Incorporation experiments: The efficiency of incorporation of the catalyst in the vesicles was measured by gel permeation chromatography (GPC) in combination with UV/Vis spectroscopy. Vesicle solutions were prepared as described above and were passed over a Sephadex G50 column with ethylmorpholine buffer as the eluent. The fractions were collected and the UV/Vis absorption spectra were measured to calculate the manganese(III) porphyrin, **Rh-5**, and amphiphile concentrations.

Electron microscopy: For the visualization of the vesicles, the negative staining method was used. A droplet of a vesicle solution was placed on a Formvar-coated copper grid which had first been made hydrophilic by exposure to an argon plasma for 2 min. After allowing adsorption on the grid to proceed for 2 min, the solution was drained with filter paper and the samples were stained with an aqueous uranyl acetate solution (1 wt%) which was removed after 1 min.

Differential scanning calorimetry: Cups containing about 10 mg of material were placed in the DSC apparatus, and heating and cooling scans were recorded with a scan rate of 2 °C min^{-1}.

Cyclic voltammetry: All measurements were carried out in water with a basal-plane pyrolytic graphite electrode as the working electrode, which was polished with alumina, rinsed with water, and cleaned in a bath-type sonicator for 1 min before use. The reference electrode was a sodium-saturated calomel electrode (SSCE), which was separated from the solution by a salt bridge of similar composition and pH; the auxiliary electrode was a platinum electrode. In a typical experiment, 4 mL of an ethylmorpholine buffered (50 mM, pH 7.0) vesicle solution of **Rh-5** and surfactant was placed in the electrochemical cell, and the solution was purged with nitrogen for 20 min. Unless otherwise indicated, the scan rate was 100 mV s^{-1}. A nitrogen stream was passed over the solution during the measurements. After the cyclic voltamograms had been recorded, ferrocenecarboxylic acid was added to give a concentration of 5×10^{-4} mol L^{-1}. The redox potential of this compound ($E_{1/2}$ = 0.275 V vs. SCCE, ΔE_p = 62 mV and i_b/i_f = 1) was measured, and the half-wave potentials are reported relative to this internal standard.

Reduction experiments: The desired amounts of stock solutions of **Rh-5**, manganese(III) porphyrin, and DHP, DODAC, DPPA, or DPPC in chloroform were mixed in a test tube. The solvent was evaporated under a stream of nitrogen to leave a homogeneous film. This film was dissolved in ethanol/tetrahydrofuran (100 μL; 1/1, v/v) and injected into water (1.25 mL) at 75 °C. The suspension was purged with argon for 30 min and injected into a cuvette containing an ethylmorpholine/sodium formate buffer (1.25 mL) at 75 °C. The course of the reaction was monitored by measuring the change of the absorbance in the UV/Vis spectrum (λ): **Rh-5** (522), **Mn-1** (435), **Mn-2** (440), **Mn-3** (453), **Mn-4** (446 nm).

Conditions: *Rhodium reduction*: 72 μM of **Rh-5**, 926 μM of surfactant in ethylmorpholine (50 mM)/sodium formate (150 mM) buffer. The resulting curves were fitted with the following first-order equation $[Rh^I]_t = [Rh^I]_{max} - [Rh^I]_{max}e^{-kt}$.

pH Experiments: 7.2 μM of **Rh-5**, 910 μM surfactant in ethylmorpholine (50 mM)/sodium formate (150 mM) buffer adjusted to the desired pH value with a concentrated sodium hydroxide solution. The pH curves were fitted with the equation $[Rh^I]_t = [Rh^I]_{max}/(K_a[H^+] + 1)$.

Formate experiments: 2.4 μM of **Mn-1**, 12 μM of **Rh-5**, 910 μM of surfactant in ethylmorpholine (50 mM)/sodium formate (varied between 0.016 and 0.150 M) buffer (pH 7.0).

Temperature experiments: 2.4 μM of **Mn-1**, 7.2 μM of **Rh-5**, 910 μM of surfactant in ethylmorpholine (50 mM)/sodium formate (150 mM) buffer (pH 7.0); *T* was varied between 25 °C and 65 °C.

Experiments with rhodium complexes: 2.4 μM of **Mn-1**, 2.4 *n* μM of **Rh-5** (*n* = Rh/Mn molar ratio), 910 μM of surfactant in ethylmorpholine (50 mM)/sodium formate (150 mM) buffer (pH = 7.0), *T* = 48 °C.

Oscillation experiment: 2.4 μM of **Mn-1**, 24.0 μM of **Rh-5**, 910 μM of DPPC in ethylmorpholine (50 mM)/sodium formate (150 mM) buffer (pH 7.0), *T* = 48 °C.

Epoxidation experiments: Final conditions: 2.4 μM of **Mn-1**, 2.4 *n* μM of **Rh-5** (*n* = Rh/Mn molar ratio), 3.5 μM of *N*-methylimidazole and 910 μM of surfactant in ethylmorpholine (50 mM)/sodium formate (250 mM) buffer (pH 7.0), 200 μM of substrate. The 100 μL of solution containing all components was directly injected into a buffered solution (2.5 mL) above the phase-transition temperature of the vesicle bilayers. After 1 min the substrate was injected, and the reaction mixture was analyzed by taking 0.2 mL aliquots, to which was added 0.1 mL of diethyl ether containing mesitylene as an internal standard. This mixture was vortexed and centrifuged. After phase separation, a 5 μL sample was taken from the diethyl ether layer and analyzed by GLC (temperature program 70 °C (2 min), 10 °C min^{-1}, 220 °C (2 min)). Reaction products were identified by GC/MS and by comparison with authentic samples.

Acknowledgments: The authors thank Dr. J. H. van Esch, Dr. M. J. B. Hauser (Universität Würzburg, Germany) and M. C. P. F. Driessen for help and stimulating discussions. This work was supported by the Dutch Foundation for Chemical Research (SON) with financial aid from the Dutch Organization for Scientific Research (NWO).

Received: October 13, 1997 [F853]

[1] F. P. Guengerich, *J. Biol. Chem.* **1991**, *266*, 10019.
[2] I. Tabushi, *Coord. Chem. Rev.* **1988**, *86*, 1.
[3] a) J. P. Collman, X. Zhang, V. J. Lee, E. S. Uffelman, J. I. Brauman, *Science* **1993**, *261*, 1404; b) B. Meunier, *Chem. Rev.* **1992**, *92*, 1411; c) D. Ostovic, T. C. Bruice, *Acc. Chem. Res.* **1992**, *25*, 314; d) S. E. J. Bell, P. R. Cooke, P. Inchley, D. R. Leanord, J. R. Lindsay Smith, A. Robbins, *J. Chem. Soc. Perkin Trans. 2* **1991**, 549.
[4] a) J. T. Groves, T. E. Nemo, R. S. Meyers, *J. Am. Chem. Soc.* **1979**, *101*, 1032; b) C. K. Chang, M.-S. Kuo, *ibid.* **1979**, *101*, 3413; c) D. Mansuy, P. Battioni, J.-P. Renaud, *J. Chem. Soc. Chem. Commun.* **1984**, 1235; d) P. N. Balsubramanian, A. Sinha, T. C. Bruice, *J. Am. Chem. Soc.* **1987**, *109*, 1456; e) R. F. Parton, I. F. J. Vankelecom, M. J. A. Casselman, C. P. Bezoukhanova, J. B. Uytterhoeven, P. A. Jacobs, *Nature*

1994, *370*, 541; f) E. Guilmet, B. Meunier, *Tetrahedron Lett.* **1980**, 4449; g) J. T. Groves, Y. Watanabe, *J. Am. Chem. Soc.* **1986**, *108*, 507.
[5] a) D. Mansuy, M. Fontecave, J.-F. Bartoli, *J. Chem. Soc. Chem. Commun.* **1983**, 253; b) I. Tabushi, A. M. Yazaki, *J. Am. Chem. Soc.* **1981**, *103*, 7371; c) P. Battioni, J.-F. Bartoli, P. Leduc, M. Fontecave, D. Mansuy, *J. Chem. Soc. Chem. Commun.* **1987**, 791; d) M. Perree-Fauvet, A. Gaudemer, *ibid.* **1987**, 874.
[6] A. B. Sorokin, A. M. Khenkin, S. A. Marakushev, A. A. Shilov, A. A. Shteinman, *Dokl. Phys. Chem.* **1984**, *29*, 1101.
[7] J. H. van Esch, M. F. Roks, R. J. M. Nolte, *J. Am. Chem. Soc.* **1986**, *108*, 6093.
[8] a) J. T. Groves, R. Neumann, *J. Am. Chem. Soc.* **1989**, *111*, 2900; b) J. T. Groves, S. B. Ungashe, *ibid.* **1990**, *112*, 7796.
[9] P. A. Gosling, J. H. van Esch, M. A. M. Hoffmann, R. J. M. Nolte, *J. Chem. Soc. Chem. Commun.* **1993**, 472.
[10] Parts of this work have been reported in short communications: a) A. P. H. J. Schenning, D. H. W. Hubert, J. H. van Esch, M. C. Feiters, R. J. M. Nolte, *Angew. Chem.* **1994**, *106*, 2587; *Angew. Chem. Int. Ed. Engl.* **1994**, *33*, 2468; b) A. P. H. J. Schenning, J. H. Lutje Spelberg, M. C. P. F. Driessen, M. J. B. Hauser, M. C. Feiters, R. J. M. Nolte, *J. Am. Chem. Soc.* **1995**, *117*, 12655.
[11] J. H. van Esch, M. A. M. Hoffman, R. J. M. Nolte, *J. Org. Chem.* **1995**, *60*, 1599.
[12] M. Caffrey, G. W. Feigenson, *Biochemistry* **1984**, *23*, 323.
[13] Y. Lei, J. K. Hurst, *J. Phys. Chem.* **1991**, *95*, 7819.
[14] R. W. Murray in *Electroanalytical Chemistry*, *Vol. 13* (Ed.: A. J. Bard), Marcel Dekker, New York, **1984**, p. 191.
[15] T. Lu, T. M. Cotton, J. K. Hurst, D. H. P. Thompson, *J. Electroanal. Chem.* **1988**, *246*, 337.
[16] T. Kunitake, *Stud. Org. Chem.* **1983**, *13*, 147.
[17] T. Lu, T. M. Cotton, J. K. Hurst, D. H. P. Thompson, *J. Phys. Chem.* **1988**, *92*, 6981.
[18] R. Ruppert, S. Herrmann, E. Steckhan, *J. Chem. Soc. Chem. Commun.* **1988**, 1150.
[19] U. Kölle, M. Grätzel, *Angew. Chem.* **1987**, *99*, 572; *Angew. Chem. Int. Ed. Engl.* **1987**, *26*, 567.
[20] M. S. Fernandez, P. Fromherz, *J. Phys. Chem.* **1977**, *81*, 1755.
[21] C. J. Drummond, F. Grieser, T. W. Healy, *J. Chem. Soc. Faraday Trans 1* **1989**, *85*, 521.
[22] B. C. Patterson, D. H. Thompson, J. K. Hurst, *J. Am. Chem. Soc.* **1988**, *110*, 3656.
[23] C. Walsh, *Acc. Chem. Res.* **1980**, *13*, 148.
[24] T. Bockman, J. Kochi, *J. Org. Chem.* **1990**, *55*, 4127.
[25] For $CaCl_2$-induced vesicle fusion, see D. Papahadjopoulos, W. J. Vail, W. A. Pangborn, G. Poste, *Biochim. Biophys. Acta*, **1976**, *448*, 265.
[26] A. P. H. J. Schenning, D. H. W. Hubert, M. C. Feiters, R. J. M. Nolte, *Langmuir* **1996**, *12*, 1572.
[27] The observation that the reduction of the porphyrin is independent of the position in the bilayer differs from earlier observations on the reduction of nicotinamides and porphyrins by Rh^{III} hydride covalently anchored to polymerized vesicles.[11] In the latter case the reaction rate did depend on the location of the substrate, and a difference in the rate of reduction in the aqueous phase and in the bilayers was found: porphyrins in the aqueous phase were reduced in a zero-order reaction, and the rate was independent of the surfactant/rhodium ratio, whereas porphyrins that were covalently linked to the vesicle bilayers were reduced in a first-order reaction, and the reaction rate did not depend on the rhodium concentration. The difference may be due to the fact that the rhodium complexes were covalently anchored to the bilayers in the earlier work.
[28] A. Lekebusch, A. Förster, F. W. Schneider, *J. Phys. Chem.* **1995**, *99*, 681.
[29] X. H. Mu, F. A. Schultz, *Inorg. Chem.* **1995**, *34*, 3835.
[30] A. W. Van der Made, R. J. M. Nolte, *J. Mol. Catal.* **1984**, *26*, 333.
[31] L. F. Fieser, *J. Am. Chem. Soc.* **1926**, *48*, 2926.
[32] J. Kaminska, M. A. Schwegeler, A. J. Hoefnagel, H. van Bekkum, *Recl. Trav. Chim. Pays-Bas* **1992**, *111*, 432.
[33] A. W. Van der Made, R. J. M. Nolte, W. Drenth, *Recl. Trav. Chim. Pays-Bas* **1988**, *107*, 15.
[34] J. H. van Esch, M. C. Feiters, A. M. Peters, R. J. M. Nolte, *J. Phys. Chem.* **1994**, *98*, 5541.
[35] A. D. Adler, F. Longo, L. F. Kampas, J. Kim, *J. Inorg. Nucl. Chem.* **1970**, *32*, 2443.
[36] A. Harriman, G. Porter, *J. Chem. Soc. Faraday Trans. 2* **1979**, 1532.
[37] A. M. Carmona-Ribeiro, H. Chaimovich, *Biochim. Biophys. Acta* **1983**, *733*, 172.
[38] R. R. C. New, *Liposomes*, *a Practical Approach* (IRL Press, Oxford University Press) **1989**, p. 8.
[39] A. M. Carmona-Ribeiro, S. Hix, *J. Phys. Chem.* **1991**, *95*, 1812.

0947-6539/98/0405-0880 $ 17.50+.50/0